

SCIENTIFIC REPORTS



OPEN

Optogenetic silencing of nociceptive primary afferents reduces evoked and ongoing bladder pain

Vijay K. Samineni^{1,2}, Aaron D. Mickle^{1,2}, Jangyeol Yoon³, Jose G. Grajales-Reyes¹, Melanie Y. Pullen¹, Kaitlyn E. Crawford³, Kyung Nim Noh³, Graydon B. Gereau^{1,2}, Sherri K. Vogt^{1,2}, H. Henry Lai^{2,4}, John A. Rogers^{3,5,6} & Robert W. Gereau IV^{1,2}

Patients with interstitial cystitis/bladder pain syndrome (IC/BPS) suffer from chronic pain that severely affects quality of life. Although the underlying pathophysiology is not well understood, inhibition of bladder sensory afferents temporarily relieves pain. Here, we explored the possibility that optogenetic inhibition of nociceptive sensory afferents could be used to modulate bladder pain. The light-activated inhibitory proton pump Archaeorhodopsin (Arch) was expressed under control of the sensory neuron-specific sodium channel (*sns*) gene to selectively silence these neurons. Optically silencing nociceptive sensory afferents significantly blunted the evoked visceromotor response to bladder distension and led to small but significant changes in bladder function. To study of the role of nociceptive sensory afferents in freely behaving mice, we developed a fully implantable, flexible, wirelessly powered optoelectronic system for the long-term manipulation of bladder afferent expressed opsins. We found that optogenetic inhibition of nociceptive sensory afferents reduced both ongoing pain and evoked cutaneous hypersensitivity in the context of cystitis, but had no effect in uninjured, naïve mice. These results suggest that selective optogenetic silencing of nociceptive bladder afferents may represent a potential future therapeutic strategy for the treatment of bladder pain.

Interstitial cystitis/bladder pain syndrome (IC/BPS) is a debilitating pelvic pain syndrome of unknown etiology^{1,2}. IC/BPS patients experience chronic pelvic pain symptoms, including pain on bladder filling, increased urinary urgency and frequency as the primary clinical symptoms^{3–12}. Blocking afferent drive from the bladder by instillation of local anesthetics has long been known to reduce bladder pain in many patients with IC/BPS^{13,14}. More targeted desensitization of C-fiber afferents using resiniferatoxin (a potent TRPV1 agonist) has also been demonstrated to reduce bladder pain in IC/BPS patients, suggesting that targeted strategies to silence bladder nociceptive afferents hold promise for the clinical management of IC/BPS^{15,16}.

The TTX-resistant sodium channel Scn10a (Nav1.8) is expressed in nociceptor populations that respond predominantly to capsaicin and inflammatory mediators^{17–19}. Additionally, C-fiber bladder afferent neurons that express Scn10a exhibit increased excitability after induction of cystitis^{20–22}. Recent studies demonstrate that rodents in which Scn10a gene is deleted or suppressed exhibit diminished bladder nociceptive responses and referred hyperalgesia after induction of cystitis^{23,24}. These results suggest that selective silencing of nociceptive sensory afferents could be an effective strategy for treating inflammation-induced bladder pain. To further study

¹Washington University Pain Center and Department of Anesthesiology, St. Louis, MO, 63110, USA. ²Washington University School of Medicine, 660 S. Euclid Ave, Box 8054, St. Louis, MO, 63110, USA. ³Department of Materials Science and Engineering, University of Illinois at Urbana-Champaign, Urbana, Illinois, 61801, USA. ⁴Washington University Department of Surgery - Division of Urologic Surgery, St. Louis, MO, 63110, USA. ⁵Department of Civil and Environmental Engineering, Mechanical Engineering, Materials Science and Engineering, Northwestern University, Evanston, IL, 60208, USA. ⁶Departments of Materials Science and Engineering, Biomedical Engineering, Chemistry, Mechanical Engineering, Electrical Engineering and Computer Science, and Neurological Surgery, Center for Bio-Integrated Electronics, Simpson Querrey Institute for Nano/biotechnology, Northwestern University, Evanston, IL, 60208, USA. Vijay K. Samineni and Aaron D. Mickle contributed equally to this work. Correspondence and requests for materials should be addressed to R.W.G. (email: gereaur@wustl.edu)

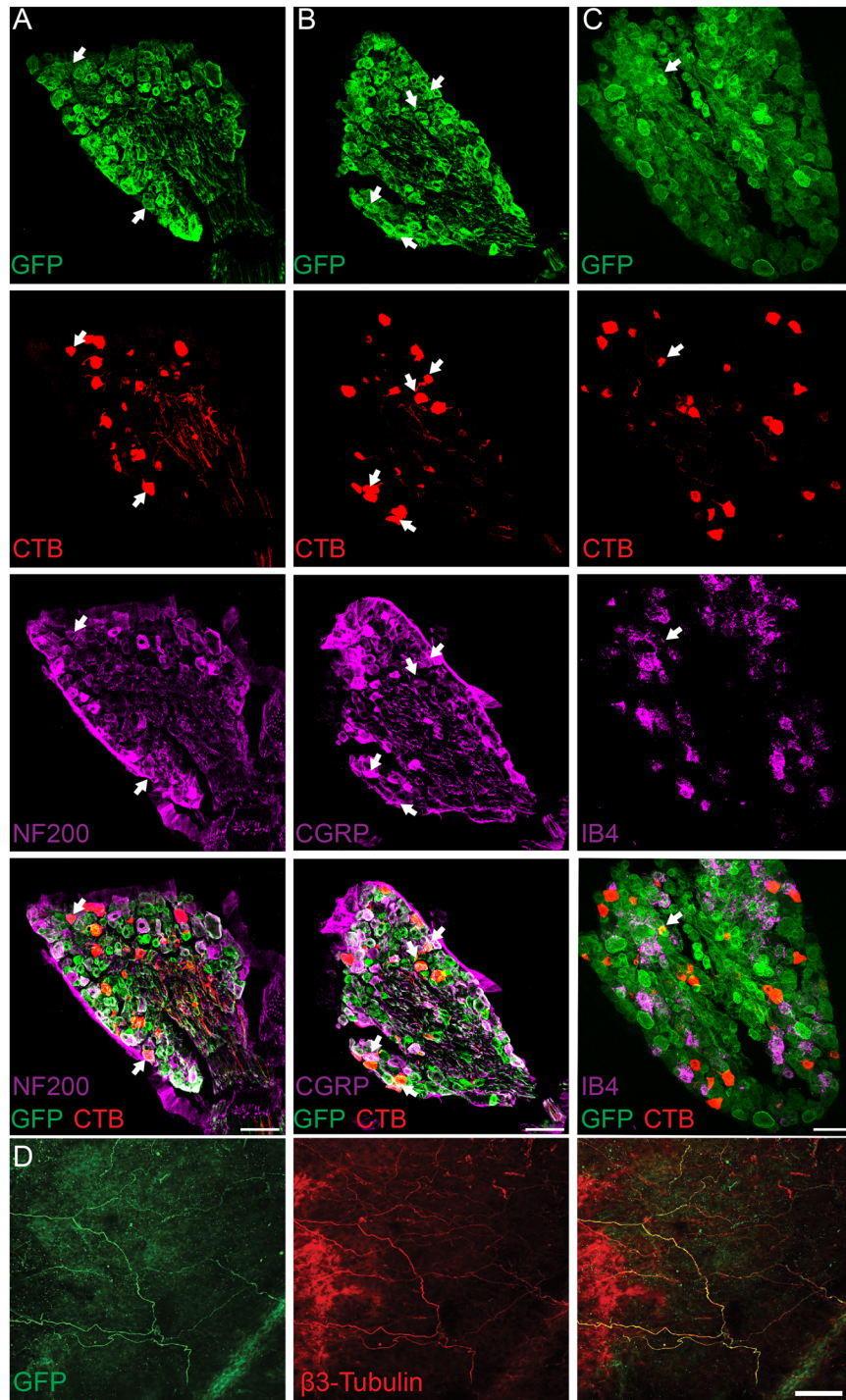


Figure 1. Histological characterization of L6-S1 dorsal root ganglion (DRG) neurons that project to the bladder from SNS-Arch mice. (**A,B & C**) Immunohistochemical analysis of tissue from SNS-Arch mice confirms GFP reporter expression in L6-S1 DRGs. Labeling of bladder-innervating DRG neurons was achieved via bladder injections of the retrograde neuronal tracer cholera toxin B. Co-labeling of GFP and CTB-555 with the neuronal markers calcitonin gene related peptide (CGRP), neurofilament 200 (NF200) and isolectin B4 (IB4) reveal a mixed population of sensory neurons that innervate the mouse bladder; scale bar 100 μm ($n = 2$). (**D**) Whole mount staining of the bladder wall shows sensory neurons expressing GFP innervate the bladder wall of SNS-Arch mice and co-label with $\beta 3$ -tubulin; scale bar 100 μm .

the role of nociceptive-specific bladder afferents we took advantage of optogenetic techniques that can specifically and reversibly inhibit these neurons.

Archaeorhodopsin (Arch) is a light-activated proton pump, which upon activation by green light (520–590 nm) induces membrane hyperpolarization and robustly suppresses neuronal firing²⁵. Previous studies have shown

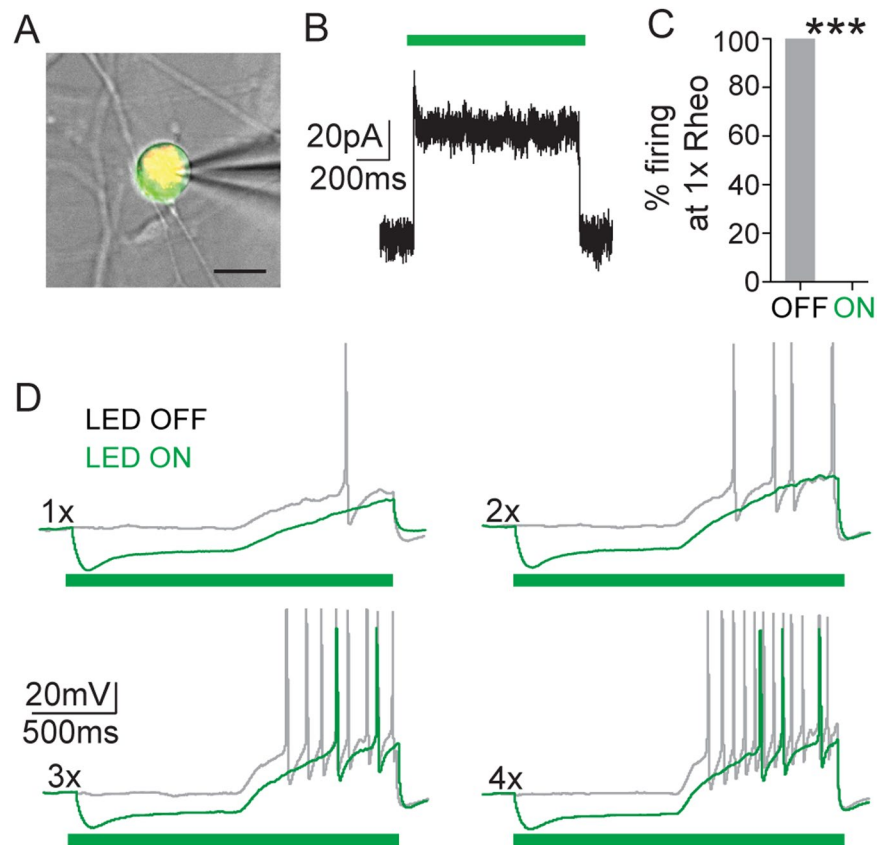


Figure 2. Arch activation in bladder sensory neurons decreased neuronal excitability. (A) Example of a patched neuron (21 μm diameter); green fluorescence indicates Arch-GFP expression, red fluorescence is DiI labeling, indicating that the neuron projects to the bladder wall and expressed Arch (yellow); scale bar = 20 μm . (B) Representative voltage clamp recording showing photocurrent elicited by 1-second green light (530 nm) stimulation at 10 mW/mm^2 . (C) Quantification of the percentage of cells that showed action potential firing to a ramp current to 1x rheobase before (OFF) and during (ON) green light illumination. Optical illumination of bladder projecting SNS-Arch neurons resulted in complete blockade of action potential firing at 1x rheobase. (D) Representative traces of action potentials elicited in SNS-Arch-GFP-expressing neurons by ramp current injections of 1 to 4 times rheobase without (grey) and with (green) LED illumination. *** $p = 0.001$. $n = 7$ neurons from 4 mice; Paired t test. Error bars indicate SEM.

that transdermal illumination of Arch expressed in nociceptive peripheral nerve terminals innervating the paw results in a significant decrease in somatic pain, suggesting that optogenetics can be used to effectively silence the peripheral nociceptors during chronic pain^{26,27}. Whether this approach can be extended to modulation of visceral pain is not known. Here, we test the hypothesis that Arch expression in nociceptive sensory neurons can reduce bladder pain in the cyclophosphamide (CYP)-induced cystitis model of bladder pain in mice.

A major challenge in applying optogenetics to studies of viscera is achieving robust and consistent light delivery to the end organ in awake and behaving animals. Recent advances in wireless optoelectronics have made it possible to activate opsins expressed in the brain, spinal cord and peripheral neurons in freely moving animals^{28–30}. Here, we have developed ultra-miniaturized, optoelectronic devices that contain micro-scale light emitting diodes (μ -ILEDs) capable of wireless operation through near field communication (NFC) hardware. This device is designed to illuminate bladder afferents (or other visceral structures) of freely moving mice. In this study, we utilize these new devices to investigate whether optical silencing of nociceptive bladder sensory neurons can attenuate ongoing pain and referred visceral hyperalgesia associated with development of CYP-induced cystitis in freely moving animals.

Results

Immunohistochemical and electrophysiological characterization of SNS-Arch expressing bladder sensory afferents.

We expressed Arch-GFP in nociceptive bladder afferents using the SNS-Cre BAC transgenic mouse line, which expresses Cre under the regulation of *Scn10a* (Nav1.8) promoter elements³¹. To determine the distribution of SNS-Arch-GFP⁺ in bladder projecting DRG neurons, we injected retrograde tracer cholera toxin subunit B (CTB) into the bladder wall of SNS-Arch mice. Seven days after CTB injection, dorsal root ganglia (DRG) at L6-S1 levels exhibited numerous CTB⁺ neurons (Fig. 1A–C). Quantitative analysis revealed that $75.2 \pm 5.2\%$ of CTB⁺ bladder projecting DRG neurons co-label with Arch-GFP. Amongst the

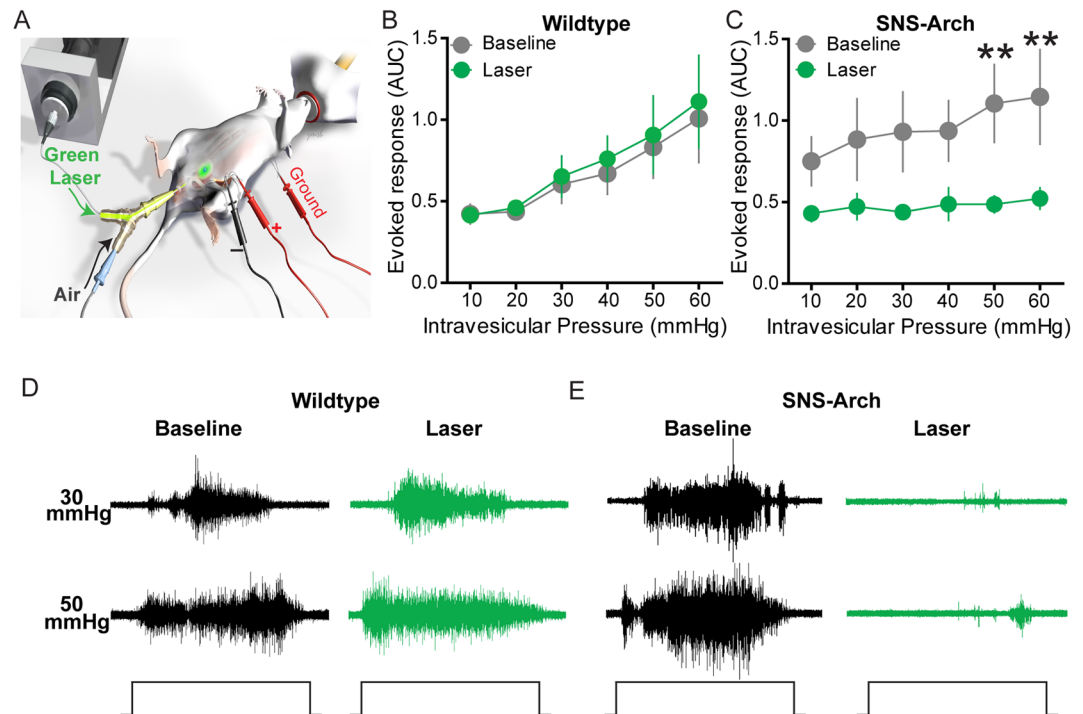


Figure 3. Optical silencing of nociceptive bladder afferents attenuates bladder nociception. (A) Schematic illustrating bladder distention (VMR) setup to optically silence bladder afferents. (B & C) Transurethral fiber optic delivery of green light to the bladder lumen to induce optical silencing of bladder afferents significantly attenuated the evoked response to 50 and 60 mmHg bladder distention compared with baseline (pre-laser) responses in SNS-Arch mice (** $p < 0.05$, $n = 12$; $F(1, 110) = 11.31$), but had no effect in wild type mice ($p > 0.05$, $n = 12$; $F(1, 110) = 0.7119$). (D & E) Representative images of raw EMG traces from wild type and SNS-Arch mice during 30 and 60 mmHg bladder distention taken before (baseline) and during (laser) green light illumination. ** $p < 0.05$, $n = 12$ mice per group; $F(1, 110) = 11.31$, Two-way ANOVA. Error bars indicate SEM. Illustration created by Janet Sinn-Hanlon, The DesignGroup@VetMed, University of Illinois at Urbana-Champaign.

CTB⁺ bladder-projecting DRG neurons that express SNS-Arch-GFP, $42 \pm 10.9\%$ are NF200-positive (Fig. 1A), $41 \pm 0.1\%$ are CGRP-positive (Fig. 1B) and $15 \pm 5.3\%$ are IB4-positive (Fig. 1C). Whole mount staining of the bladder wall of SNS-Arch mice showed that Arch-GFP-positive fibers co-label with the neuronal marker $\beta 3$ -tubulin, suggesting that Arch-GFP is effectively transported to afferent endings in the bladder (Fig. 1D).

We performed whole-cell patch clamp electrophysiology recordings on cultured DRG neurons from SNS-Arch mice to verify functional expression of Arch in nociceptive bladder sensory afferents. We identified bladder-projecting DRG neurons using the retrograde dye, DiI, injected into the bladder wall and then recorded from bladder-projecting (DiI⁺, red) and Arch-GFP⁺ (green) cell bodies (Fig. 2A). In voltage clamp, illumination of Arch-GFP-expressing bladder projecting neurons with green light (530 nm) induced robust outward currents (Fig. 2B). This current was sufficient to suppress action potential firing in response to ramp current injections in all neurons tested (Fig. 2C,D; *** $p = 0.001$, $n = 7$ neurons from 4 mice; Paired t test).

Optogenetic inhibition of bladder sensory afferent terminals attenuates distension-induced nociception and voiding behavior.

We next tested if inhibition of nociceptive bladder sensory afferents could attenuate bladder nociception in response to distension. Bladder nociception was assessed from the abdominal muscles by electromyogram (EMG) recordings evoked by bladder distention (10–60 mmHg distention in 10 mmHg steps, as we have described previously^{32,33}). This EMG response is called the visceromotor response (VMR) and is a validated approach to measuring bladder distension-induced nociception in rodents^{32,34,35}. Effects of light-dependent inhibition of nociceptive bladder afferents on bladder nociception were tested by inserting a fiber optic cable via a “Y” tube that enabled delivery of compressed air to distend the bladder and light to illuminate the lumen of the bladder (Fig. 3A). In control mice, transurethral illumination with green light had no effect on the evoked VMR to bladder distention (Fig. 3B,D). However, in SNS-Arch mice, transurethral illumination suppressed the distension-induced VMR compared to pre-illumination baseline VMR (Fig. 3C,E, $p < 0.05$, $n = 12$ mice per group; two-way ANOVA). These results suggest that optogenetic inhibition of nociceptive bladder sensory afferents can attenuate bladder distension evoked nociception.

We tested whether optogenetic inhibition of bladder sensory afferents influences urodynamics by performing cystometric analysis of bladder function before and during laser illumination of the bladder (Fig. 4A). In anesthetized wild type and SNS-Arch mice, illumination of bladder afferents with green light did not significantly alter maximum pressure, baseline pressure or threshold pressure (Fig. 4B,C). However, we did observe a slight

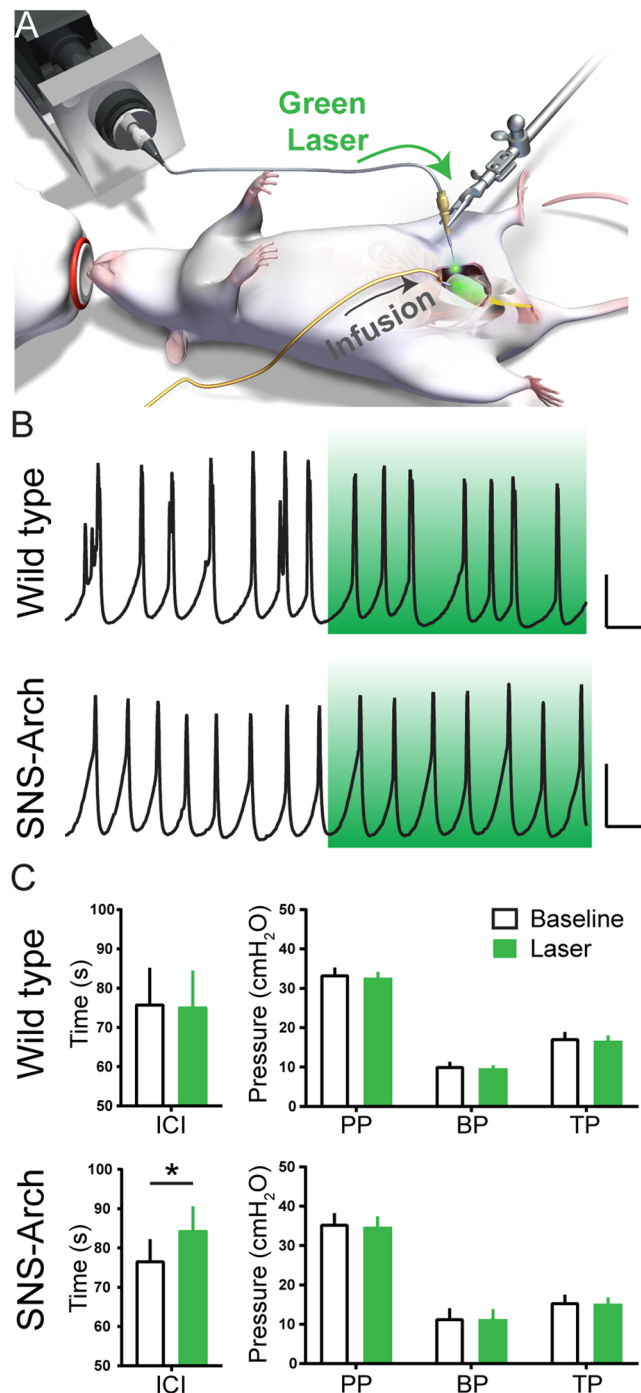


Figure 4. Effect of Arch induced inhibition of nociceptive on cystometric function. **(A)** Schematic illustrating cystometry setup using fiber optic to activate Arch in bladder sensory neurons. **(B)** Example cystometric traces recorded from wild type (top) and SNS-Arch mice (bottom). Scale bars are 10 seconds and 100 cmH₂O. **(C)** Quantification of peak pressure (PP), base pressure (BP), threshold pressure (TP) and intercontraction interval (ICI) of wild type and SNS-Arch mice before and during laser illumination of bladder. ICI was significantly increased during laser illumination in SNS-Arch but not in wild type mice. * $p = 0.008$. $n = 7-8$ mice per group; Paired t test. Error bars indicate SEM. Illustration created by Janet Sinn-Hanlon, The DesignGroup@VetMed, University of Illinois at Urbana-Champaign.

(10.96%), yet statistically significant increase in the intercontraction interval (ICI) during laser illumination of the bladder in SNS-Arch mice compared to baseline, an effect that was absent in control mice (Fig. 4B,C; * $p = 0.008$, $n = 7-8$ mice per group; Paired t test).

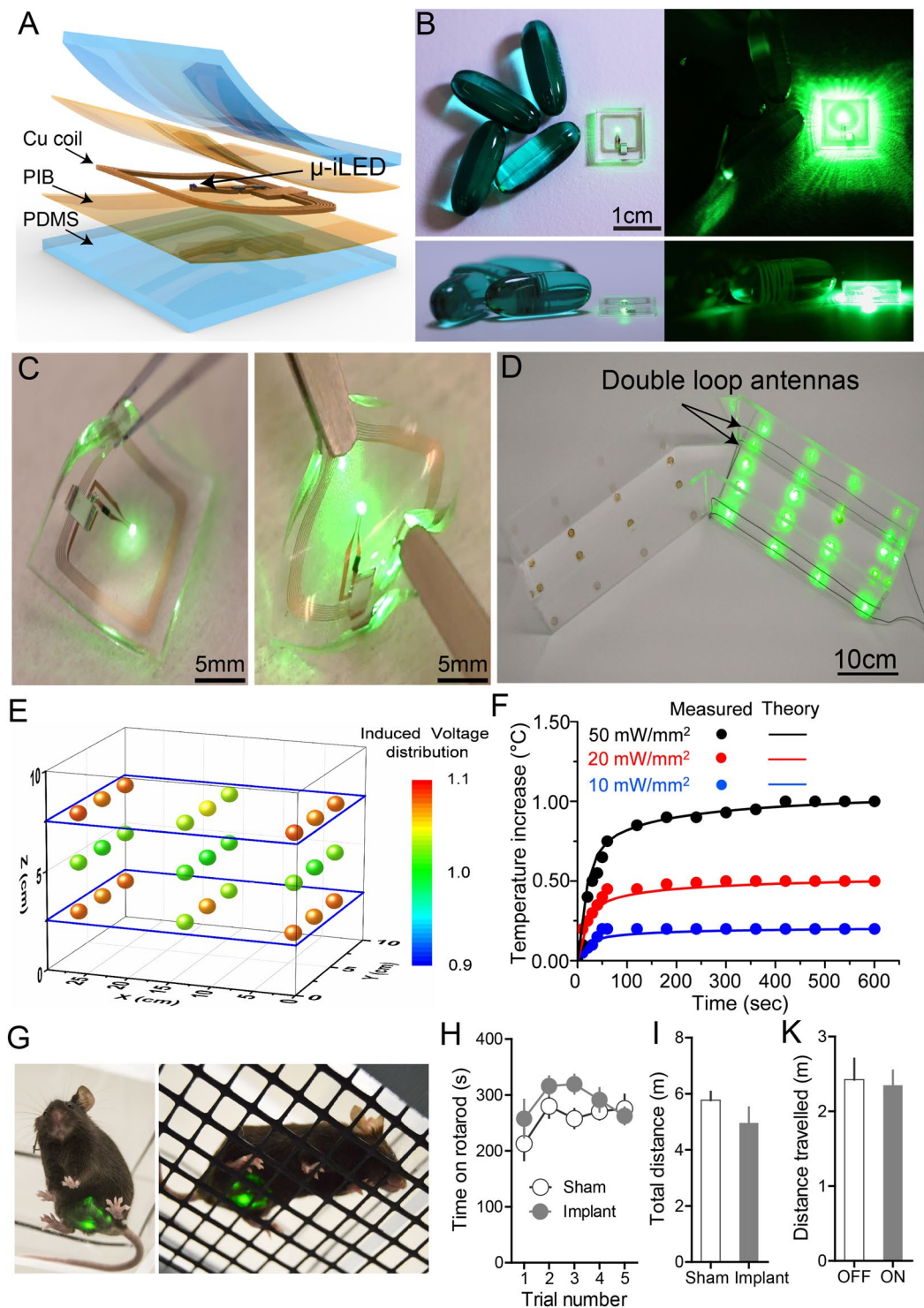


Figure 5. Flexible wireless optoelectronic device designed for optogenetic modulation of bladder afferent neurons. **(A)** Schematic illustration of the layered conformation of optoelectronic device. **(B)** Image of a micro-fabricated device adjacent to a 200 g capsules for the size comparison. **(C)** Demonstration of the flexibility of a functioning device with a forceps. **(D)** Image of wireless operation of optoelectronic devices in the V-maze with the double loop antennas. **(E)** Measurement of the normalized output power distribution of nine devices at heights of 2.5, 5, and 7.5 cm from the bottom of the cage demonstrating uniform power distribution of across the cage. **(F)** Thermal modeling and management of a μ -iLED device versus time at different peak output powers (20, 50, and 100 mW/mm^2) demonstrating a maximum of 1 degree change at maximum light output of 100 mW/mm^2 . **(G)** Mice with wireless optoelectronic devices implanted over the bladder. **(H)** Implantation of the bladder optoelectronic device did not effect on motor behavior vs. sham animals in the rotarod test ($P = 0.12$, $F_{4,4} = 1.118$, $t_{1,8} = 1.407$ $n = 8$ sham, $n = 8$ device). **(I)** Mice with bladder implants did not exhibit

significant difference in total distance travelled in open field test compared to sham mice ($P = 0.16$, two-tailed, $n = 8$ sham, $n = 8$ device). (K) There is no difference in distance traveled between an NFC-On and NFC-Off chamber in wild type mice. ($P = 0.8556$, two-tailed, $n = 12$ wild type,).

Development of a wireless optoelectronic device to enable optogenetic manipulation of bladder afferents in awake, freely moving animals. While the results above suggest that silencing nociceptive bladder afferents could affect bladder nociception and function, it is possible that the anesthetics used in these studies could interfere with nociceptive processing. Currently, we lack technology to optically activate opsins expressed in the bladder afferents and determine their necessity in mediating bladder pain in awake, freely moving animals. We overcame this barrier by adapting technology that we have recently developed^{28,30}, to fabricate a flexible optoelectronic device to specifically target light to the lower abdomen. These devices are powered by near field communication (NFC) technology to achieve robust wireless functionality for chronic applications and for use in a wide variety of behavioral arenas (Fig. 5A). These wireless optoelectronic devices consist of a conductive metal pattern (18 μm thickness copper foil), semiconducting components (μ -ILED/mounted chips), with an encapsulation bilayer of polyisobutylene (PIB, 5 μm) and polydimethylsiloxane (PDMS, 500 μm). The electrical system incorporates a rectangular coil (width: 8 mm, length: 8 mm, copper traces: 7 turns with 70 μm width and 30 μm adjacent spacing) with surface mounted chips for power transfer via magnetic control to a loop antenna operating at 13.56 MHz. The overall dimensions of the device are 1 cm \times 1 cm \times 1 mm ($l \times w \times t$, Figure 5B), which is depicted next to 200 mg capsules. An image of the device bent with forceps (Fig. 5C) demonstrates the device flexibility and functionality in the bent conformation which enables interfacing with the abdominal wall. The thin-film PIB provides a protective barrier against moisture to allow for long-term use in a dynamic cage environment³⁶. This PIB barrier allowed for 100% of the devices to function for at least 4 weeks after implantation in the animal, with more than 50% of devices remaining functional after 6 months and some devices still functional at > 9 months after implantation.

These small and flexible optoelectronic devices can be adapted to a wide array of behavioral or home cage environments by tuning flexible signal antennas specifically for the dimensions of the behavioral or home cage environment. Figure 5D shows an example of the experimental setup for power transmission from antenna to optoelectronic devices in a V-maze (experimental data in Fig. 6B and C). The double-loop antenna is installed around the perimeter of one arm of the maze; for optimal power output performance, the loop antennae are placed 2.5 cm and 7.5 cm from the bottom of the cage. The spatial uniformity of power is demonstrated by equal illumination of twelve optoelectronic devices placed at different locations in a V-maze cage (Fig. 5D). This antenna configuration also allows for uniform μ -ILED illumination on the vertical dimension as well, which is important for maintaining consistent illumination during mouse rearing (Fig. 5E). The output power is normalized by its value at the center of double loop antenna at 5 cm and provides evidence that deviation of output power from the double loop antenna is less than 20%. This result indicates that the position of the double-loop antennas allows for a uniform magnetic field within the cage. This powering scheme allows for consistent and uniform illumination of implanted μ -ILEDs, which is critically important to reduce variability in light delivery during optogenetic experiments. A limitation of this powering scheme is a loss of power when the device is angled more than 45 degrees³⁰. To avoid any issues with reduced efficiency of powering, we ensured that mice were not rearing when we tested mechanical sensitivity.

We also determined the heat generation under operation conditions by measuring the temperature at the surface of the device, in the mouse as a function of time, at peak output powers of 20 mW/mm^2 , 50 mW/mm^2 , and 100 mW/mm^2 . Measured values show good agreement with the thermal modeling, as shown in Fig. 5F (symbols: measured values, lines; simulated theoretical values). The temperature approaches 'steady-state' after 5 min with a temperature increase of only 0.5 $^{\circ}\text{C}$ after 10 min at an output power of 50 mW/mm^2 . Mice with implanted NFC devices over the bladder exhibited no significant difference in locomotor function in the Rotarod test or in the open field test compared to sham-operated controls, suggesting that these devices do not impair motor behavior or coordination in freely moving animals (Fig. 5G–I). Additionally, there was no significant difference in distance traveled in NFC-on vs a NFC-off chamber in wild type mice. Thus, device implantation and activation has no detectable effect on motor behavior.

Wireless optogenetic inhibition of nociceptive bladder sensory afferents reduces pain behaviors in a mouse model of bladder pain.

Using the implantable optoelectronic devices described above, we evaluated the effects of optically inhibiting nociceptive bladder sensory afferents on referred abdominal sensitivity in awake, freely moving mice with CYP-induced cystitis. We have previously reported that patients with IC/BPS demonstrate referred hyperalgesia to the suprapubic region of the abdomen³⁷. Numerous studies have demonstrated that this referred hypersensitivity is reproduced in mouse models of bladder pain, including the CYP model^{32,37–44}. As it is not currently possible to induce bladder distension to measure VMR in awake (un-anesthetized) freely moving animals, we chose to test whether this referred abdominal hypersensitivity induced by CYP could be suppressed by inactivation of nociceptive bladder sensory afferents. SNS-Arch or wild type mice were implanted with wireless μ -ILED devices subcutaneously in the abdomen, with the μ -ILED positioned to illuminate the bladder through the abdominal musculature (Fig. 5G). After baseline assessments of cutaneous mechanical sensitivity, measured by application of von Frey filaments to the lower abdomen, mice were given a single injection of CYP (200 mg/kg, i.p), which induced robust referred mechanical hyperalgesia compared to baseline measurements (Fig. 6A,B) (pre-CYP, Fig. 6A, **** $p < 0.0001$ comparing naïve to post-CYP, $n = 11$ mice per group, two-way ANOVA). Activation of the optoelectronic devices implanted over the bladder had no effect on abdominal sensitivity in either wild type or SNS-Arch mice in the naïve state. However, optical

inhibition of bladder sensory afferents significantly reduced the abdominal hypersensitivity induced by CYP ($\#p < 0.05$, $n = 6$ mice per group, two-way ANOVA), an effect that is absent in wild type mice (Fig. 6A,B). The inhibition of nociceptive sensory afferents in CYP-treated mice reduced abdominal mechanical sensitivity to values comparable to that of the baseline sensitivity (pre-CYP).

The results above demonstrate that referred mechanical hyperalgesia (von Frey filament experiments) can be reversed by optogenetic inhibition of nociceptive bladder afferents. However, the primary complaint of IC/BPS patients is not referred hypersensitivity, but ongoing pain and pain associated with bladder filling^{37,45}. It is difficult to quantify ongoing pain in animals; in fact, it is not even clear if animals with CYP-induced cystitis exhibit ongoing pain. Development of these wireless optoelectronic devices presents us with the opportunity to evaluate ongoing, non-evoked visceral pain. We hypothesize that if silencing nociceptive bladder afferents relieves ongoing bladder pain, then this should result in positive reinforcement (reward) on activation of the μ -ILED device. We can measure positive reinforcement using a real-time place preference (RTPP) assay, in which animals are placed in a V maze, with free access to roam throughout the maze. In one arm of the maze, NFC induces μ -ILED device activation (LED ON), while in the other arm, devices are inactive (LED OFF; Fig. 5D). Thus, in the LED ON arm, nociceptive bladder afferents (which express Arch) are inhibited, and in the LED OFF arm, they can fire action potentials normally. If silencing nociceptive bladder afferents relieves ongoing bladder pain, animals should demonstrate a preference for the LED ON arm compared to the LED OFF arm. In the naïve state, both wild type and SNS-Arch mice exhibited no preference for either the LED ON or LED OFF arms (SNS-Arch LED ON vs LED OFF, $p = 0.6606$, $n = 6$ mice per group, two-way ANOVA) (Fig. 6C,E). However, after CYP-induced cystitis, SNS-Arch mice showed significant RTPP for the LED ON arm compared to the LED OFF arm, whereas wild type mice with CYP-induced cystitis show no preference (SNS-Arch LED ON vs LED OFF, $^{##}p = 0.0065$, $n = 11$ mice per group, two-way ANOVA) (Fig. 6D–F). These results suggest that inhibition of nociceptive bladder sensory afferents attenuates both ongoing pain and referred abdominal hypersensitivity in a mouse model of bladder pain.

Discussion

The cardinal clinical symptoms of IC/BPS include pain upon bladder filling (distention) and inhibiting bladder sensory afferents can reduce this pain in many patients. Prior studies have demonstrated that the majority of bladder-projecting C-fiber neurons express Nav1.8-mediated Na^{2+} currents^{20,46}. In addition, C-fiber bladder afferents that express Nav1.8 channels are known to exhibit increased excitability in animal models of bladder pain, suggesting the importance of these afferents in mediating bladder nociception^{23,24}. We confirmed the assumptions made by these original studies^{23,24} by specifically inhibiting nociceptive bladder afferents with the inhibitory channel Arch expressed under the control of the SNS promoter and demonstrated that these fibers play a critical role in bladder nociception and a minor role in bladder voiding.

Previous studies have shown that C-fibers are silent during normal bladder distension and can become active during bladder injury. Thus, C-fiber activity is thought to contribute to bladder nociception in response to injury and have a sparse role in innocuous sensation of the bladder under normal physiological conditions^{20,46–49}. Consistent with these reports, we find that inhibition of nociceptive bladder afferents bladder sensory afferents significantly attenuates nociception related to bladder injury induced by CYP and has no effect in naïve mice.

Somewhat surprisingly, in our cystometry studies, we found that silencing nociceptive bladder sensory afferents resulted in a small yet significant increase in the ICI in naïve SNS-Arch mice. The first possible explanation for this is that the relatively non-physiological, rapid rate of bladder filling in continuous flow cystometry engages nociceptive afferents to a small degree and inhibition of these afferents leads to delays in ICI. Alternatively, the effect of silencing SNS-Arch⁺ afferents on bladder function may not be due to Arch expression in small diameter nociceptors. SNS-Cre lineage neurons include a majority of C-fibers and also a smaller population of NF200⁺ A-fibers⁵⁰. Indeed, consistent with a previous study⁵⁰, we demonstrate that a proportion of bladder-projecting SNS-Cre⁺ neurons co-express NF200 (myelinated sensory neurons). It is possible that these cells include low threshold mechanoreceptors, which are known to be involved in the voiding reflex^{51,52}. Thus, this population of NF200⁺ bladder afferents might contribute to the delay in ICI we observe after optically silencing SNS-Arch⁺ bladder afferents.

A limitation of using VMR to measure bladder nociception is that these experiments must be performed in lightly anesthetized mice, and the response is evoked with invasive bladder distention. The fully implantable wireless NFC-powered μ -ILED devices we developed offer the ability to optically control neural activity in awake (un-anesthetized) and freely behaving mice. This allows us to determine the effects of silencing nociceptive bladder sensory afferents in both normal and pathological states. Optical silencing of nociceptive bladder afferents resulted in attenuation of referred mechanical hypersensitivity induced by CYP, while there were no effects of green light in naïve mice. This result suggests that in the context of bladder pain, hyperactivity in the nociceptive afferents mediates referred mechanical hypersensitivity. One limitation of this experiment is that we cannot be certain whether silencing nociceptive bladder afferents or nociceptive cutaneous afferents resulted in this attenuation of referred mechanical hypersensitivity, as light from our devices could also inhibit cutaneous abdominal afferents over the device. Nonetheless, these studies demonstrate that nociceptive afferents are critical for the mechanical hypersensitivity evoked by the CYP model of bladder pain.

While IC/BPS patients demonstrate referred hypersensitivity, the primary clinical complaint is spontaneous pain and pain on bladder filling^{37,45,53}. Reflexive measurements of referred hypersensitivity do not assess whether the ongoing bladder pain induced by cystitis is being relieved. It is possible, for example, that silencing nociceptive bladder afferents attenuates mechanical hypersensitivity but does not reduce ongoing pain associated with bladder filling. We employed a RTPP paradigm to evaluate whether silencing the nociceptive bladder afferents causes relief of spontaneous or ongoing bladder pain. Inhibition of nociceptive bladder afferents produced robust

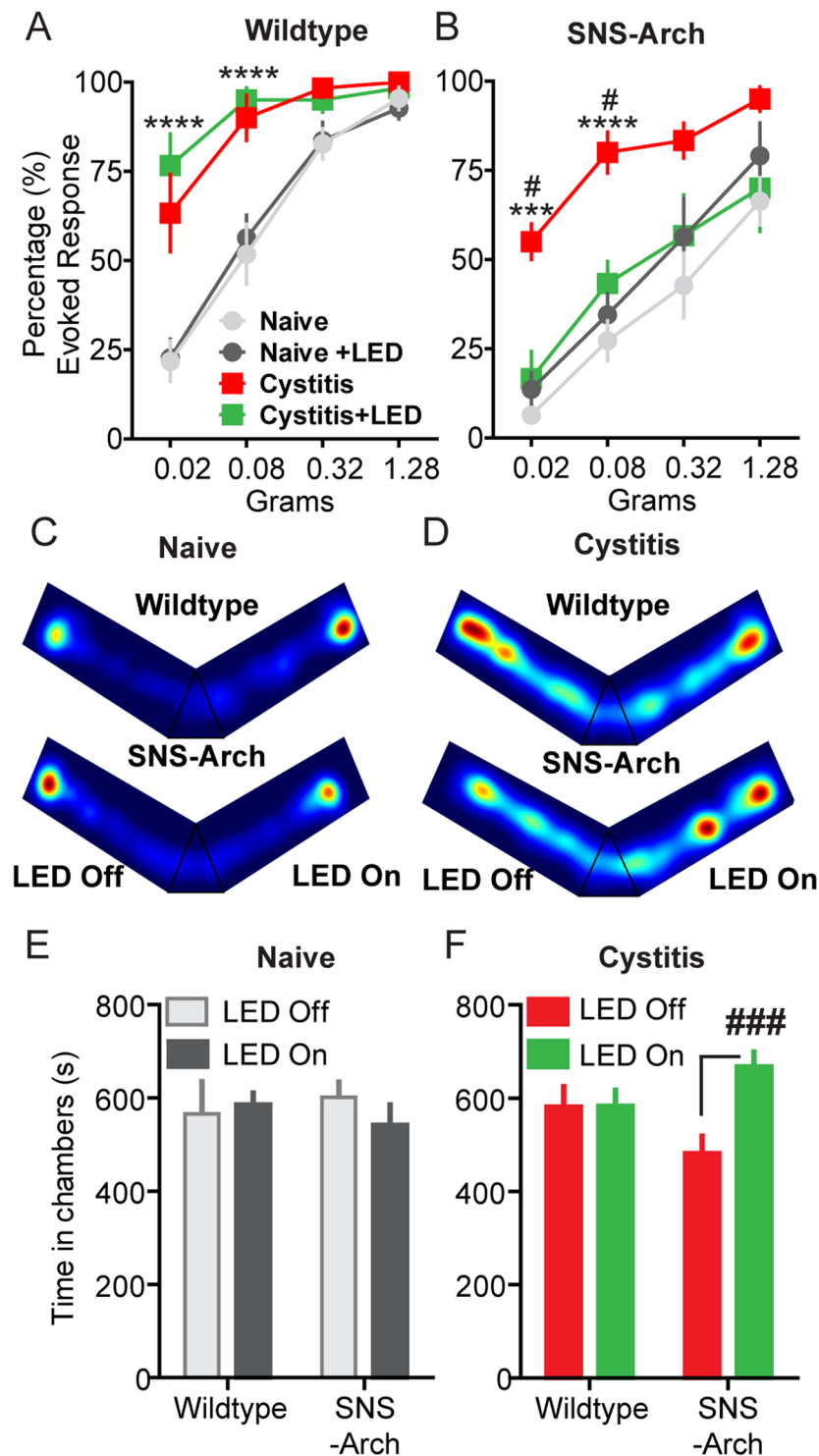


Figure 6. Optical silencing of nociceptive bladder afferents attenuates evoked and ongoing bladder nociception. Quantification of abdominal mechanical sensitivity, measured by counting evoked responses to a series of von Frey filaments with increasing force before and during CYP-induced cystitis. (A) In wild type mice, activation of wireless μ -ILEDs had no significant effect on evoked responses in the naïve state compared to their baseline values. CYP (200 mg/kg i.p.) resulted in a significant increase in abdominal sensitivity. Activation of the optoelectronic devices implanted over bladder had no effect on abdominal sensitivity after cystitis ($****p < 0.0001$ comparing naïve to post-CYP, $F(3, 90) = 76.31$, $n = 11$ mice per group, two-way ANOVA). (B) In SNS-Arch mice, activation of wireless μ -ILEDs had no significant effect on evoked responses in the naïve state compared to their baseline values. After cystitis induction, optical inhibition of nociceptive sensory afferents significantly attenuated the abdominal hypersensitivity to values comparable to that of the baseline sensitivity recorded before CYP treatment ($*p < 0.05$, $****p = 0.0006$, $F(3, 30) = 7.596$; $****p < 0.0001$, $F(3, 90) = 67.17$, $n = 11$ mice per group, two-way ANOVA). (C and D) Representative heat maps displaying time

spent each zone of the custom V-maze in naïve (C) and cystitis (D) mice. Red indicates areas where the animals spend a higher proportion of their time. (E) In naïve conditions (pre-CYP), both wild type and SNS-Arch mice did not exhibit any preference for either LED-ON or LED-OFF chamber ($F_{1,8} = 0.21$, $p = 0.6606$, $n = 6$ mice per group, two-way ANOVA). (F) After cystitis induction, SNS-Arch mice showed significant RTPP to the LED-ON arm compared to the LED-OFF arm, whereas wild type mice have no preference ($F_{1,18} = 9.47$, $^{***}p = 0.0065$, $n = 11$ mice per group, two-way ANOVA). Error bars indicate SEM.

RTPP in mice with cystitis, but not in uninjured mice without any cystitis. This result suggests that CYP-induced cystitis indeed induces ongoing pain, and that relief of this ongoing pain is analgesic and rewarding as evident by robust RTPP. To our knowledge this is the first demonstration of optogenetic inhibition of primary afferent neurons reducing spontaneous or ongoing bladder pain, or pain of any origin.

Combining cell type specific optogenetic inhibitory opsins with fully implantable wireless μ -ILEDs offers insights into the potential application of optogenetic neuromodulation to the treatment of pathological pain. To achieve clinical translatability of optogenetics, several obstacles remain, including the development of viral gene therapy vectors that are safe and effective for use in humans. It is vital to develop a robust vector that can efficiently target a large number of bladder afferents, but at the same time achieve cell type-specific targeting, as this could help reduce unwanted side effects. However, assessment of potential toxicities associated with long-term expression of opsins in neurons will be critical. Additionally, chronic studies are needed to determine what effects long-term optogenetic inhibition has on sensory neurons and if these opsins would remain effective over extended use. Promising advances have been made in gene therapy by targeting neurons using viral vectors, but much work must be done to advance this to the clinical arena. Combining any of these gene therapy approaches that prove to be safe with real-time control of neural dynamics with closed-loop optoelectronic systems^{54–57} could lead to the development of future therapies for bladder pain and/or voiding dysfunction. While the μ -ILED technology demonstrated here would need additional modifications to meet the requirements of the clinical setting (thicker tissue and different powering schemes), the present results provide a proof of concept and suggest that optogenetic silencing of nociceptive bladder afferents could be an effective approach to alleviate pain associated with IC/BPS.

Materials and Methods

Animals and genetic strategy. All experiments were performed in accordance with the National Institute of Health guidelines and received the approval of the Animal Care and Use Committee of Washington University School of Medicine. Adult mice (8–12 weeks of age) were used for this study. Mice were housed in the animal facilities of the Washington University School of Medicine on a 12 h light/dark cycle, with ad libitum access to food and water. Experiments were performed on male heterozygous SNS-Cre mice³¹ crossed to female homozygous Gt(ROSA)26Sor^{tm35.1(CAG-aop3/GFP)Hze} (Ai35) mice from Jackson Laboratory carrying floxed stop-Arch-GFP gene in the Gt(ROSA)26Sor locus⁵⁸ to generate the SNS-Arch mouse line. The SNS-Cre mice are a BAC transgenic line, where the endogenous Nav1.8 locus is not altered. While these mice are known to express Cre in all Nav1.8⁺ neurons, not all Cre-expressing cells express Nav1.8 in adult mice^{50,59,60}. These mice express Cre in majority of nociceptive C-fibers and also a smaller population of A-fibers⁵⁰. We used wildtype C57BL/6J mice in our study to control for effects of the LED implants or light/illumination in each experiment. We are not directly comparing Bl6/C57 animals to the SNS-Arch mice. All animals are used as their own controls, comparing the effects before and during light/illumination.

Immunohistochemistry. Immunohistochemistry was performed using the same methods as Park *et al.*²⁸. Briefly, DRG tissue was collected 7 days after Cholera Toxin Subunit B Alexa Fluor[®] 555 (Thermo Fischer Scientific, C22843) injection. Tissues were fixed with 4% PFA and then embedded with O.C.T. Compound (Tissue-Tek, 4583) for sectioning. Tissues were washed in PBS and incubated in blocking solution (10% normal goat serum/0.1% Triton-X/1x PBS) for 1 hour at room temperature. Primary antibodies (1:200 Mouse anti-CGRP, Sigma C7113; 1:200 Mouse anti-NF200, Sigma N0142; 1:1000 Rabbit anti-GFP, Thermo Fischer A11122), or IB4 (1:100, IB4 Alexa Fluor 647, Thermo Fischer I32450) were diluted in blocking solution and incubated on the sections overnight. Slides were washed 3x for 10 min each with PBS and incubated with secondary antibodies diluted in blocking solution for 1 hour at room temperature (1:1000 Goat anti-mouse IgG Alexa Fluor 647, Thermo Fischer A-21235; 1:1000 Goat anti-rabbit IgG Alexa Fluor 488, Thermo Fischer A11008). Slides were washed 3x for 10 min each with PBS, and allowed to dry before mounting coverslips (Vectashield Hard Set, H-1400). Samples were imaged using a Leica TCS SP5 confocal microscope. For more detailed methods see supplementary methods.

Dorsal root ganglion (DRG) culture and whole-cell electrophysiology. DRG culture and whole cell recordings were performed as in Park *et al.*²⁸. Briefly, DRG neurons were dissociated from mice 7 days after Dil (ThermoFisher) injection. Neurons were recorded and optically stimulated with an EPC10 amplifier (HEKA Instruments) and Patchmaster software (HEKA Instruments). Optical stimulation was delivered through the microscope objective, using a custom set-up with a green (530 nm) LED (M530L3; Thorlabs). Light intensity of the LED at the focal plane was 10 mW/mm². For more detailed methods see supplementary methods.

Visceromotor reflex behavior. The visceromotor reflex (VMR) in female mice was quantified using abdominal electromyograph (EMG) responses. The VMR is a reliable behavioral index of visceral nociception in rodents and was performed as previously described^{34,35,61–63}. Briefly, mice were anesthetized with isoflurane (2% in oxygen) and silver wire electrodes were placed in the oblique abdominal muscle. A lubricated,

24-gauge angiocatheter was passed into the bladder via the urethra for urinary bladder distension (UBD). After surgical preparation, isoflurane was reduced to ~1% until a flexion reflex response was present (evoked by pinching the paw), but righting reflex was absent. Phasic UBD consisted of graded distensions at pressures of 10–60 mmHg. Baseline EMG activity was subtracted from EMG during UBD, rectified, and integrated to obtain distension-evoked EMG responses. Distension-evoked EMG is presented as area under the curve. Experimenters were blinded to mouse genotype. For more detailed methods see supplementary methods.

Cystometry. Mice (6.5–11 weeks old) were first anesthetized with isoflurane (2%), then a midline incision was used to expose the bladder dome. Isoflurane was used to replicate the anesthesia levels used to record the VMR. A 25-gauge butterfly needle was used to puncture the dome of the bladder and warm mineral oil placed on the exposed bladder to prevent tissue drying. After the catheter was placed, anesthesia was lowered to 1.5% for 1 hour. Then over 30–40 minutes, the anesthesia was slowly reduced to ~0.8%. At this point, bladders were filled at 0.04 ml/min with room-temperature water or saline (no differences observed between fluids; data not shown) using a syringe pump to evoke a regular voiding pattern. Intravesicular pressure was measured using a pressure transducer amplified by a Transbridge transducer amplifier (WPI) and recorded using WINDAQ data acquisition software (DataQ Instruments) at a sampling rate of 5 Hz. After a regular voiding pattern was established, a ten-minute baseline was collected followed by laser illumination (described below) for at least ten minutes and a ten-minute recovery period. The laser was always turned on at the end of a contraction and then off at the end of a contraction resulting in some trials that were greater than ten-minutes. These trials were completed in duplicate for each animal and parameters were averaged. Data were analyzed using a Matlab (Mathworks) script to determine base pressure (BP), threshold pressure (TP), maximum pressure (MP) and intercontraction interval (ICI) (terminology conformed to⁶⁴). All data files were blinded so analysis could occur in an unbiased manner.

Photoinhibition of VMR and Cystometry. Optical inhibition of VMR was performed using a 532 nm, 200 mW diode-pumped solid-state (DPSS) laser. In visceromotor reflex studies, a fiber optic (200 μ m diameter core; BFH48–200–Multimode, NA 0.48; Thorlabs) was coupled to the laser and connected to the transurethral catheter via a Y-shaped connector. The fiber tip was positioned 0.1 mm beyond the tip of the catheter in the bladder lumen. Photoinhibition was performed at 10 mW/mm² constant illumination. For cystometry, photoinhibition was performed with the same fiber optic positioned above the exposed bladder dome instead of transurethrally and at 30 mW/mm² constant illumination.

NFC device fabrication. Micro-fabrication of the soft, flexible wireless optoelectronic devices started with a spin-cast poly(dimethylsiloxane) (PDMS, Sylgard 184) at 600 RPM \times 60 sec on a clean glass slide (75 \times 50 \times 1 mm, L \times W \times thickness), followed by curing at 150 $^{\circ}$ C \times 10 min. Next, an 8% by weight solution of polyisobutylene (PIB, BASF) in heptane was applied to freshly cured PDMS by spin-casting at 1000 RPM \times 60 sec followed by a 3 min bake at 100 $^{\circ}$ C. Then copper foil (18 μ m thickness) was placed on the newly formed polymer substrate. Photolithography (AZ 4620, AZ Electronic Materials) and copper etching was then used to define the conducting pattern. Next, the electronic components (μ -ILED (TR2227, 540 nm, Cree Inc. Raleigh, NC), rectifier (CBDQR0130L-HF, Comchip Technology, Fremont, CA), and 136 pF capacitor (GRM1555C1H680JA01J, Murata electronics, Japan)) were placed onto the copper pattern using conductive paste. Then a second layer of polyisobutylene was added to the device, followed by another PDMS layer, using the same conditions described above.

Implantation of wireless NFC device. The NFC optoelectronic devices were used to activate Arch in freely moving mice. Under isoflurane anesthesia, a small incision was made in the abdominal skin and the device was implanted subcutaneously between the skin and muscle, positioned to illuminate the lower abdomen and bladder. The incision was then closed using surgical staples. The animals were allowed to recover for at least 4 days before behavioral experiments were performed.

Cyclophosphamide (CYP) induced cystitis. Cyclophosphamide (CYP) was used to induce bladder inflammation and visceral pain. Bladder cystitis was initiated by a single injection of CYP (200 mg/kg; i.p; Sigma, St. Louis) dissolved in saline. Behavioral assays were performed before (baseline), 4 and 24 hours after CYP injection.

Abdominal mechanical sensitivity. Abdominal sensitivity was measured by counting the number of withdrawal responses to 10 applications of von Frey filaments (North Coast Medical, Inc, Gilroy, CA; 0.02, 0.08, 0.32 and 1.28 g) to the lower abdomen. Each mouse was allowed at least 15 seconds between each application and at least 5 minutes between each size filament. Animals were acclimated to individual boxes on a plastic screen mesh for at least one hour before testing. All experimenters were blinded to mouse genotype and treatment. NFC devices were activated by an antenna wrapped around the individual cage, prior to the experiment the antenna was tested to insure full NFC coverage of the cage. NFC antenna power and signal were generated by Neurolux hardware and software (Neurolux, Urbana, IL).

Real-time place preference (RTPP). Place preference was tested in a custom made V-maze constructed of plexiglass with a layer of corn cob bedding. Each arm of the two-arm V maze is 10 cm wide \times 30 cm long \times 10 cm height neutral area between arms. To generate the NFC signal, one arm of the maze was covered with an NFC-emitting antenna (Neurolux, Urbana, IL) allowing for the control of μ -ILED devices throughout one arm of the maze. To begin the experimental protocol, a mouse was placed in the neutral area of the maze and was continuously monitored and recorded through a video connection for 20 min. Ethovision software (Noldus, Leesburg, VA.) was used to determine time-in-chamber and generate representative heat maps for each condition.

Statistics. Results are expressed as means \pm SEM. Mann-Whitney test was used to compare the percentage suppression of action potentials and cytometric parameters. To analyze VMR and mechanical sensitivity data, two-way ANOVA with repeated measures was used. Bonferroni's *post hoc* tests were used (when significant main effects were found) to compare effects of variables (genotype, treatment). A value of $p < 0.05$ was considered statistically significant for all statistical comparisons. Researchers were blinded to all experimental conditions. Two replicate measurements were performed and averaged in all behavioral assays.

Data availability. The datasets generated during and/or analyzed during the current study are available from the corresponding author on reasonable request.

References

- Rosenberg, M. T., Page, S. & Hazzard, M. A. Prevalence of interstitial cystitis in a primary care setting. *Urology* **69**, 48–52 (2007).
- Berry, S. H. *et al.* Prevalence of symptoms of bladder pain syndrome/interstitial cystitis among adult females in the United States. *The Journal of urology* **186**, 540–544, <https://doi.org/10.1016/j.juro.2011.03.132> (2011).
- Hepner, K. A. *et al.* Suicidal ideation among patients with bladder pain syndrome/interstitial cystitis. *Urology* **80**, 280–285, <https://doi.org/10.1016/j.jurology.2011.12.053> (2012).
- Macaulay, A. J., Stern, R. S., Holmes, D. M. & Stanton, S. L. Micturition and the mind: psychological factors in the aetiology and treatment of urinary symptoms in women. *Br Med J (Clin ResEd)* **294**, 540–543 (1987).
- Baldoni, F., Ercolani, M., Baldaro, B. & Trombini, G. Stressful events and psychological symptoms in patients with functional urinary disorders. *Percept Mot Skills* **80**, 605–606, <https://doi.org/10.2466/pms.1995.80.2.605> (1995).
- Rothrock, N. E., Lutgendorf, S. K., Kreder, K. J., Ratliff, T. & Zimmerman, B. Stress and symptoms in patients with interstitial cystitis: a life stress model. *Urology* **57**, 422–427 (2001).
- Wu, E. Q. *et al.* Interstitial Cystitis: Cost, treatment and co-morbidities in an employed population. *Pharmacoeconomics* **24**, 55–65 (2006).
- Theoharides, T. C., Pang, X., Letourneau, R. & Sant, G. R. Interstitial cystitis: a neuroimmunoendocrine disorder. *Ann N Y Acad Sci* **840**, 619–634 (1998).
- Alagiri, M., Chottiner, S., Ratner, V., Slade, D. & Hanno, P. M. Interstitial cystitis: unexplained associations with other chronic disease and pain syndromes. *Urology* **49**, 52–57 (1997).
- Erickson, D. R., Morgan, K. C., Ordille, S., Keay, S. K. & Xie, S. X. Nonbladder related symptoms in patients with interstitial cystitis. *The Journal of urology* **166**, 557–561; discussion 561–552 (2001).
- Warren, J. W. *et al.* Evidence-based criteria for pain of interstitial cystitis/painful bladder syndrome in women. *Urology* **71**, 444–448, S0090-4295(07)02317-5 [pii] <https://doi.org/10.1016/j.jurology.2007.10.062> (2008).
- Ness, T. J., Powell-Boone, T., Cannon, R., Lloyd, L. K. & Fillingim, R. B. Psychophysical evidence of hypersensitivity in subjects with interstitial cystitis. *The Journal of urology* **173**, 1983–1987, <https://doi.org/10.1097/01.ju.0000158452.15915.e2> (2005).
- Nickel, J. C. *et al.* Intravesical alkalinized lidocaine (PSD597) offers sustained relief from symptoms of interstitial cystitis and painful bladder syndrome. *BJU international* **103**, 910–918, <https://doi.org/10.1111/j.1464-410X.2008.08162.x> (2009).
- Zhang, W., Deng, X., Liu, C. & Wang, X. Intravesical treatment for interstitial cystitis/painful bladder syndrome: a network meta-analysis. *International urogynecology journal*. <https://doi.org/10.1007/s00192-016-3079-4> (2016).
- Lazzeri, M. *et al.* Intravesical resiniferatoxin for the treatment of hypersensitive disorder: a randomized placebo controlled study. *The Journal of urology* **164**, 676–679 (2000).
- Guo, C. *et al.* Intravesical resiniferatoxin for the treatment of storage lower urinary tract symptoms in patients with either interstitial cystitis or detrusor overactivity: a meta-analysis. *PLoS one* **8**, e82591, <https://doi.org/10.1371/journal.pone.0082591> (2013).
- Akopian, A. N. *et al.* The tetrodotoxin-resistant sodium channel SNS has a specialized function in pain pathways. *Nat Neurosci* **2**, 541–548, <https://doi.org/10.1038/9195> (1999).
- Akopian, A. N., Sivilotti, L. & Wood, J. N. A tetrodotoxin-resistant voltage-gated sodium channel expressed by sensory neurons. *Nature* **379**, 257–262 (1996).
- Tanaka, M. *et al.* SNS Na⁺ channel expression increases in dorsal root ganglion neurons in the carrageenan inflammatory pain model. *Neuroreport* **9**, 967–972 (1998).
- Yoshimura, N., White, G., Weight, F. F. & de Groat, W. C. Different types of Na⁺ and A-type K⁺ currents in dorsal root ganglion neurons innervating the rat urinary bladder. *J Physiol* **494**(Pt 1), 1–16 (1996).
- Black, J. A. *et al.* Tetrodotoxin-resistant sodium channels Na(v)1.8/SNS and Na(v)1.9/NaN in afferent neurons innervating urinary bladder in control and spinal cord injured rats. *Brain research* **963**, 132–138 (2003).
- Yoshimura, N. & de Groat, W. C. Increased excitability of afferent neurons innervating rat urinary bladder after chronic bladder inflammation. *J Neurosci* **19**, 4644–4653 (1999).
- Yoshimura, N. *et al.* The involvement of the tetrodotoxin-resistant sodium channel Na(v)1.8 (PN3/SNS) in a rat model of visceral pain. *J Neurosci* **21**, 8690–8696 (2001).
- Laird, J. M., Souslova, V., Wood, J. N. & Cervero, F. Deficits in visceral pain and referred hyperalgesia in Nav1.8 (SNS/PN3)-null mice. *J Neurosci* **22**, 8352–8356 (2002).
- Chow, B. Y. *et al.* High-performance genetically targetable optical neural silencing by light-driven proton pumps. *Nature* **463**, 98–102, <https://doi.org/10.1038/nature08652> (2010).
- Iyer, S. M. *et al.* Virally mediated optogenetic excitation and inhibition of pain in freely moving nontransgenic mice. *Nat Biotechnol* **32**, 274–278, <https://doi.org/10.1038/nbt.2834> (2014).
- Daou, I. *et al.* Optogenetic Silencing of Nav1.8-Positive Afferents Alleviates Inflammatory and Neuropathic Pain. *eNeuro* **3**, <https://doi.org/10.1523/ENEURO.0140-15.2016> (2016).
- Park, S. I. *et al.* Soft, stretchable, fully implantable miniaturized optoelectronic systems for wireless optogenetics. *Nat Biotechnol* **33**, 1280–1286, <https://doi.org/10.1038/nbt.3415> (2015).
- Montgomery, K. L. *et al.* Wirelessly powered, fully internal optogenetics for brain, spinal and peripheral circuits in mice. *Nature methods* **12**, 969–974, <https://doi.org/10.1038/nmeth.3536> (2015).
- Shin, G. *et al.* Flexible Near-Field Wireless Optoelectronics as Subdermal Implants for Broad Applications in Optogenetics. *Neuron* **93**, 509–521 e503, <https://doi.org/10.1016/j.neuron.2016.12.031> (2017).
- Agarwal, N., Offermanns, S. & Kuner, R. Conditional gene deletion in primary nociceptive neurons of trigeminal ganglia and dorsal root ganglia. *Genesis* **38**, 122–129 (2004).
- Lai, H. *et al.* Animal Models of Urologic Chronic Pelvic Pain Syndromes: Findings From the Multidisciplinary Approach to the Study of Chronic Pelvic Pain Research Network. *Urology* **85**, 1454–1465, <https://doi.org/10.1016/j.jurology.2015.03.007> (2015).
- Lai, H. H. *et al.* Activation of spinal extracellular signal-regulated kinases (ERK) 1/2 is associated with the development of visceral hyperalgesia of the bladder. *Pain* **152**, 2117–2124, <https://doi.org/10.1016/j.pain.2011.05.017> (2011).
- Ness, T. J. & Elhefni, H. Reliable visceromotor responses are evoked by noxious bladder distention in mice. *The Journal of urology* **171**, 1704–1708, <https://doi.org/10.1097/01.ju.0000116430.67100.8f> (2004).

35. Ness, T. J., Lewis-Sides, A. & Castroman, P. Characterization of pressor and visceromotor reflex responses to bladder distention in rats: sources of variability and effect of analgesics. *The Journal of urology* **165**, 968–974 (2001).
36. French, R. H. *et al.* Degradation science: Mesoscopic evolution and temporal analytics of photovoltaic energy materials. *Current Opinion in Solid State and Materials Science* **19**, 212–226, <https://doi.org/10.1016/j.cossms.2014.12.008> (2015).
37. Lai, H. H., Gardner, V., Ness, T. J. & Gereau, R. W. T. Segmental hyperalgesia to mechanical stimulus in interstitial cystitis/bladder pain syndrome: evidence of central sensitization. *The Journal of urology* **191**, 1294–1299, <https://doi.org/10.1016/j.juro.2013.11.099> (2014).
38. Boudes, M. *et al.* Functional characterization of a chronic cyclophosphamide-induced overactive bladder model in mice. *NeuroUrol Urodyn* **30**, 1659–1665, <https://doi.org/10.1002/nau.21180> (2011).
39. Bicer, F. *et al.* Chronic pelvic allodynia is mediated by CCL2 through mast cells in an experimental autoimmune cystitis model. *Am J Physiol Renal Physiol* **308**, F103–113, <https://doi.org/10.1152/ajprenal.00202.2014> (2015).
40. Wantuch, C., Piesla, M. & Leventhal, L. Pharmacological validation of a model of cystitis pain in the mouse. *Neurosci Lett* **421**, 250–252, <https://doi.org/10.1016/j.neulet.2007.05.043> (2007).
41. Bon, K., Lichtensteiger, C. A., Wilson, S. G. & Mogil, J. Characterization of cyclophosphamide cystitis, a model of visceral and referred pain, in the mouse: species and strain differences. *The Journal of urology* **170**, 1008–1012, <https://doi.org/10.1097/01.ju.0000079766.49550.94> (2003).
42. Galan, A., Cervero, F. & Laird, J. M. Extracellular signaling-regulated kinase-1 and -2 (ERK 1/2) mediate referred hyperalgesia in a murine model of visceral pain. *Brain Res Mol Brain Res* **116**, 126–134 (2003).
43. Warren, J. W. *et al.* Sites of pain from interstitial cystitis/painful bladder syndrome. *The Journal of urology* **180**, 1373–1377, <https://doi.org/10.1016/j.juro.2008.06.039> (2008).
44. Fitzgerald, M. P., Koch, D. & Senka, J. Visceral and cutaneous sensory testing in patients with painful bladder syndrome. *NeuroUrol Urodyn* **24**, 627–632, <https://doi.org/10.1002/nau.20178> (2005).
45. Gardella, B. *et al.* Interstitial Cystitis is Associated with Vulvodynia and Sexual Dysfunction—A Case-Control Study. *J Sex Med* **8**, 1726–1734, <https://doi.org/10.1111/j.1743-6109.2011.02251.x> (2011).
46. Masuda, N. *et al.* Characterization of hyperpolarization-activated current (I_h) in dorsal root ganglion neurons innervating rat urinary bladder. *Brain research* **1096**, 40–52, <https://doi.org/10.1016/j.brainres.2006.04.085> (2006).
47. Dmitrieva, N. & McMahon, S. B. Sensitization of visceral afferents by nerve growth factor in the adult rat. *Pain* **66**, 87–97 (1996).
48. Gold, M. S., Reichling, D. B., Shuster, M. J. & Levine, J. D. Hyperalgesic agents increase a tetrodotoxin-resistant Na⁺ current in nociceptors. *Proc Natl Acad Sci USA* **93**, 1108–1112 (1996).
49. Cardenas, C. G., Del Mar, L. P., Cooper, B. Y. & Scroggs, R. S. 5HT₄ receptors couple positively to tetrodotoxin-insensitive sodium channels in a subpopulation of capsaicin-sensitive rat sensory neurons. *J Neurosci* **17**, 7181–7189 (1997).
50. Shields, S. D. *et al.* Nav1.8 expression is not restricted to nociceptors in mouse peripheral nervous system. *Pain* **153**, 2017–2030, <https://doi.org/10.1016/j.pain.2012.04.022> (2012).
51. Djouhri, L. *et al.* The TTX-resistant sodium channel Nav1.8 (SNS/PN3): expression and correlation with membrane properties in rat nociceptive primary afferent neurons. *J Physiol* **550**, 739–752, <https://doi.org/10.1113/jphysiol.2003.042127> (2003).
52. Ho, C. & O'Leary, M. E. Single-cell analysis of sodium channel expression in dorsal root ganglion neurons. *Mol Cell Neurosci* **46**, 159–166, <https://doi.org/10.1016/j.mcn.2010.08.017> (2011).
53. Backonja, M. M. & Stacey, B. Neuropathic pain symptoms relative to overall pain rating. *J Pain* **5**, 491–497, <https://doi.org/10.1016/j.jpain.2004.09.001> (2004).
54. Grosenick, L., Marshel, J. H. & Deisseroth, K. Closed-loop and activity-guided optogenetic control. *Neuron* **86**, 106–139, <https://doi.org/10.1016/j.neuron.2015.03.034> (2015).
55. Paz, J. T. *et al.* Closed-loop optogenetic control of thalamus as a tool for interrupting seizures after cortical injury. *Nat Neurosci* **16**, 64–70, <https://doi.org/10.1038/nn.3269> (2013).
56. Yttri, E. A. & Dudman, J. T. Opponent and bidirectional control of movement velocity in the basal ganglia. *Nature* **533**, 402–406, <https://doi.org/10.1038/nature17639> (2016).
57. Newman, J. P. *et al.* Optogenetic feedback control of neural activity. *Elife* **4**, e07192, <https://doi.org/10.7554/eLife.07192> (2015).
58. Madisen, L. *et al.* A toolbox of Cre-dependent optogenetic transgenic mice for light-induced activation and silencing. *Nature neuroscience* **15**, 793–802, <https://doi.org/10.1038/nn.3078> (2012).
59. Liu, Y. *et al.* VGLUT2-Dependent Glutamate Release from Nociceptors Is Required to Sense Pain and Suppress Itch. *Neuron* **68**, 543–556, <https://doi.org/10.1016/j.neuron.2010.09.008> (2010).
60. Chiu, I. M. *et al.* Transcriptional profiling at whole population and single cell levels reveals somatosensory neuron molecular diversity. *Elife* **3**, ARTN e04660 <https://doi.org/10.7554/eLife.04660> (2014).
61. Castroman, P. & Ness, T. J. Vigor of visceromotor responses to urinary bladder distension in rats increases with repeated trials and stimulus intensity. *Neuroscience letters* **306**, 97–100 (2001).
62. Ness, T. J., Randich, A. & Gebhart, G. F. Further behavioral evidence that colorectal distension is a 'noxious' visceral stimulus in rats. *Neuroscience letters* **131**, 113–116 (1991).
63. Crock, L. W. *et al.* Metabotropic glutamate receptor 5 (mGluR5) regulates bladder nociception. *Molecular pain* **8**, 20, <https://doi.org/10.1186/1744-8069-8-20> (2012).
64. Andersson, K. E., Soler, R. & Fullhase, C. Rodent models for urodynamic investigation. *NeuroUrol Urodyn* **30**, 636–646, <https://doi.org/10.1002/nau.21108> (2011).

Acknowledgements

This work was funded by the NIH Director's Transformative Research Award (TR01 NS081707), an NIH SPARC Award via the National Institute of Biomedical Imaging And Bioengineering of the National Institutes of Health award number U18EB021793 to RWG and JAR, and R01NS42595 to RWG, Urology Care Foundation Research Scholars Program and Kailash Kedia Research Scholar award to VKS, and a McDonnell Center for Cellular and Molecular Neurobiology Postdoctoral Fellowship to A.D.M. Illustration created by Janet Sinn-Hanlon, The DesignGroup@VetMed, University of Illinois at Urbana-Champaign.

Author Contributions

V.K.S. and R.W.G. conceptualized the project; V.K.S. and A.D.M. designed, performed experiments and collected data. J.G.G. performed anatomical analysis. M.P. performed electrophysiological experiments. G.B.G. performed behavioral experiments. S.V. performed mouse genotyping. H.H.L. provided equipment for the VMR and cystometry experiments. K.N.N. provided Matlab code for cystometry data analysis. J.Y., K.C. and J.A.R. designed and provided optoelectronic devices. V.K.S., A.D.M. and R.W.G. analyzed the data and wrote the manuscript with comments from all the authors.

Additional Information

Supplementary information accompanies this paper at <https://doi.org/10.1038/s41598-017-16129-3>.

Competing Interests: JAR and RWG are co-founders of Neurolux, a company that manufactures wireless optoelectronic devices. The devices described here are similar to devices that will be produced as part of the company's portfolio.

Publisher's note: Springer Nature remains neutral with regard to jurisdictional claims in published maps and institutional affiliations.



Open Access This article is licensed under a Creative Commons Attribution 4.0 International License, which permits use, sharing, adaptation, distribution and reproduction in any medium or format, as long as you give appropriate credit to the original author(s) and the source, provide a link to the Creative Commons license, and indicate if changes were made. The images or other third party material in this article are included in the article's Creative Commons license, unless indicated otherwise in a credit line to the material. If material is not included in the article's Creative Commons license and your intended use is not permitted by statutory regulation or exceeds the permitted use, you will need to obtain permission directly from the copyright holder. To view a copy of this license, visit <http://creativecommons.org/licenses/by/4.0/>.

© The Author(s) 2017